NAZARBAYEV UNIVERSITY

ARSENIC TRIOXIDE AND D-VITAMIN C DRUG COMBINATION INDUCES OXIDATIVE STRESS AND ALTERS ELECTRON TRANSPORT CHAIN ACTIVITY OF KRAS-MUTANT CANCER CELLS

Kristina Raish
(B.Sc. in Natural Sciences, Eurasian National University)

A THESIS SUBMITTED
FOR THE DEGREE OF MASTER OF SCIENCE IN BIOLOGICAL SCIENCES
DEPARTMENT OF BIOLOGY SCHOOL OF SCIENCES AND HUMANITIES
NAZARBAYEV UNIVERSITY
2024

Student: Kristina Raish
Supervisor: Dr. Dos Sarbassov

DECLARATION

I hereby declare that the thesis is my original work and it has been written by me in its entirety. I have duly acknowledged all the sources of information which have been used in the thesis. This thesis has also not been submitted for any degree in any university previously.

Kristina Raish

19 April 2024

ACKNOWLEDGEMENTS

I would like to acknowledge my supervisor and PI of the project Professor Dos Sarbassov for his help and support. His advice and guidance caried me through the whole project till its completion. I am sincerely grateful for having an opportunity to join the Laboratory of Cell Growth Regulation where I grew up not only as a scientist but as a person as well.

I would like to give a special thanks to Doctor Agata Burska whose expertise and support had a great contribution to the current work. I hope that in the future I will still have a chance to build a fruitful collaboration which may lead to new scientific discoveries.

In addition, I want to thank all members of the Laboratory of Cell Growth Regulation which I appreciate to be a part of. I value all their help and cherish the knowledge that they kindly shared with me. On top of it, our team is not about collaboration only but friendship. Hope our relationship will remain warn and tight through our carrier path.

The most special thanks are dedicated to my family. Their emotional support helped me to stay motivated and believe in my strength. With them by my side I believe that I can become a better version of me.

TABLE OF CONTENTS

Nazarbayev University, School of Sciences and Humanities, Department of Biology
Master´s Degree Program in Biology

Kristina Raish: Arsenic Trioxide and D-Vitamin C Drug Combination Induces Oxidative Stress and Alters Electron Transport Chain Activity of KRAS-Mutant Cancer Cells.
Master of Science thesis; 43 pages, 5 appendixes
Supervisors: Dos Sarbassov, Professor, School of Sciences and Humanities, Nazarbayev University
19.04.2024

Keywords KRAS-mutant cancer, electron transport chain, ROS, mitochondria, cancer.

ABSTRACT

Mutation in Kirsten rat sarcoma (KRAS) protooncogene is implicated in about 25-30% of all human cancers. It is usually associated with aggressive tumor progression and poor prognosis. Until now targeting KRAS-mutant cancer remains quite challenging even though several approaches were applied. However, all such strategies led to drug resistance which makes it even more challenging to specifically target KRAS-mutant cancer.

Arsenic trioxide and D-Vitamin C (ATO/D-VC) is a novel approach to targeting KRAS-mutant cancer cells using vulnerabilities in their metabolism. These cells are highly sensitive to oxidative imbalance which makes them a perfect target for ATO/D-VC drug combination as it can trigger so-called suicidal reactive oxygen species production by mitochondria (SPRM). In the current study the molecular aspects of ATO/D-VC mechanism of action was explored. It was shown that downregulation of succinate dehydrogenase (complex II) of the electron transport chain might be the primary cause of SPRM triggered by the action of ATO/D-VC synergetic drug combination.

Understanding the mechanism behind SRPM is essential for comprehending the potent cytotoxicity against KRAS-mutant cancers.

ATO/D-VC oxidative drug combination showed effectiveness during Phase 1 and currently undergoes Phase 2 of clinical trials in Kazakhstan.

LIST OF TABLES

LIST OF FIGURES AND ILLUSTRATIONS

ABBREVIATIONS

ATO	arsenic trioxide
D-VC	D-vitamin C
KRAS	Kristen rat sarcoma
GTP	guanosine triphosphate
PI3K	phosphatidylinositol 3-kinases
RAF	rapidly accelerated fibrosarcoma
RalGEF	Ras-like small GTPases
SH2	Src homology 2
Grb2	growth factor receptor-bound protein 2
GEF	guanine nucleotide exchange factor
SOS-1	son of sevenless homolog 1
ROS	reactive oxygen species
OXPHOS	oxidative phosphorylation
ETC	electron transport chain
ATP	adenosine triphosphate
TCA	tricarboxylic acid
c-MYC	c-myelocytomatosis oncogene product
HIF-1α	hypoxia-inducible factor 1 alpha
NAD	nicotinamide adenine dinucleotide
FAD	flavin adenine dinucleotide
DHA	dehydroascorbate
ARD-1	arrest-defective-1 protein
pVHL	von Hippel-Lindau
PCK2	carboxykinase
LPCAT4	lysophosphatidylcholine acyltransferase
ACSL5	acyl CoA synthetase 5

1 INTRODUCTION

1.1 KRAS protooncogene and its role in tumorigenesis

1.1.1 KRAS associated signaling pathways play a crucial role in cell proliferation and survival.

Kristen rat sarcoma (KRAS) is a small GTP-ase that mediates GTP (guanosine triphosphate) to GDP (guanosine diphosphate) hydrolysis (Kim et al., 2021).

The functions and protein-to-protein interactions of the KRAS protein are highly dependent from its structural features. It is composed of G-domain with two its lobes (effector and allosteric) and hypervariable regions on carboxyl terminus where post-translational modifications take place. The effector lobe promotes the interactions with effectors such as rapidly accelerated fibrosarcoma (RAF), phosphatidylinositol 3-kinases, (PI3K), and Ras-like (Ral) small GTPases (RalGEF), whereas the allosteric lobe take part in intra-protein communication (Kim et al., 2021; Mo, Coulson, & Prior, 2018).

Switch I and switch II residues as a part of the effector lobe influences its binding to effectors and interaction with the downstream transducer molecules. In addition to it, KRAS protein has two phosphate binding loops which is a GTP-binding pocket which distinguishes it from the RAS family as well as CAXX motif mediating its localization on the plasma membrane (Kim et al., 2021) (Fig 1).

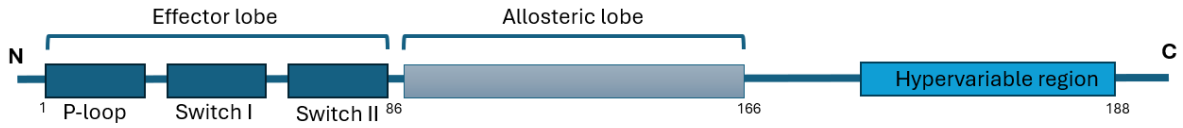

Figure 1. *Structural characteristics of KRAS protein.*

KRAS remains inactive by GDP binding and gets activated only when bound by GTP that is mediated by GTPase activator activity. In comparison to wild type KRAS, the mutant protein possesses the decreased affinity to GTPase activator proteins. In addition to it mutant KRAS shows better GTP binding rather than GDP (Kim et al., 2021, Molina & Adjei, 2006).

The activation of the wild type KRAS protein happens through the ligand binding to the tyrosine kinase receptor such as epidermal growth factor receptor (EGFR). Ligand binding triggers receptor oligomerization and transphosphorylation that is recognized by Src

homology 2 (SH2) domain of growth factor receptor-bound protein 2 (Grb2). This recognition allows guanine nucleotide exchange factor (GEFs) son of sevenless homolog 1 (SOS-1) to be recruited to the membrane and promotes the exchange of GDP for GTP in KRAS protein modulating the downstream signaling (Molina & Adjei, 2006; Ros et al., 2024). However, the preferential binding of GTP by mutant KRAS protein allows it to trigger downstream signaling without growth factor presence (Kim et al., 2021; Molina & Adjei, 2006) (Fig.2).

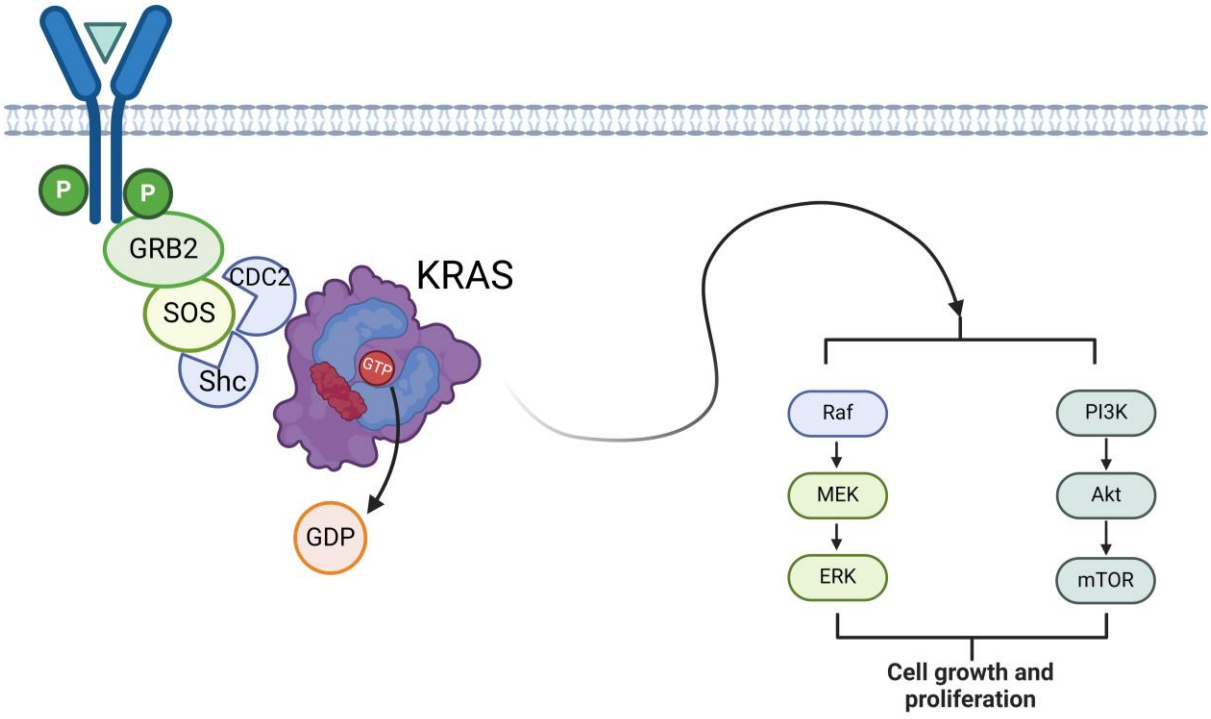

Figure 2. *Schematic representation of signaling pathways related to KRAS protein (The illustration was created using BioRender.com).*

1.2 Mitochondria, KRAS and cancer: connecting the dots.

1.2.1 The alternation of mitochondrial functions fuels cancer metabolism

Normal activity of the cell is supplied with the energy through glucose metabolism under normoxic conditions. However, for cancer cells which require high rate of biosynthetic processes metabolic rewire towards glycolysis is essential. Such metabolic shift from oxidative phosphorylation to aerobic glycolysis in cancer cells is called Warburg effect (Liberti & Locasale, 2016).

In his research, Otto Warburg clarified the significance of the decrease in respiration and inferred that the rise in lactate generation in cancer cells was a sign of a glycolytic shift. Even in the presence of oxygen, a significant portion of the glucose taken in by the tumor cells was fermented to lactate. That is referred to as "aerobic glycolysis" (Warburg, 1925). Subsequently, he deducted that all cancer cells had "injured" respiration. As a result, he started the research elucidating the precise nature of this "injury" that may cause the cells to become irreversibly damaged but not dead. The elimination of oxygen was one suggested method. He proposed that a major contributing factor to the development of cancer is oxygen shortage (Warburg, 1956). But further research on the function of growth factors in oncogenesis and their direct control over metabolism provided new insight into Warburg's hypothesis of cancer biology. Additionally, it became clear from other research that addressing mitochondrial metabolism as well as aerobic glycolysis would be necessary to halt tumor progression (Liberti & Locasale, 2016).

A significant component of the metabolic reprogramming in both pre-malignant and malignant cancers are mitochondria. Oxidative phosphorylation (OXPHOS), a process that takes place in the electron transport chain (ETC) in aerobic conditions, is how mitochondria generate cellular energy in the form of adenosine triphosphate (ATP). In contrast, glycolysis in the cytosol is the primary means of producing ATP in an anaerobic environment (Moindjie et al., 2021). Specific GLUT transporters carry glucose into the cell, where glycolysis converts it into pyruvate, which is then carried into the mitochondria where it transforms into acetyl-coA and enters the tricarboxylic acid (TCA) cycle. At the same time, glutamate produced during glutaminolysis can also supply TCA cycle activity. From this process, reduced nicotinamide adenine dinucleotide (NADH) and flavin adenine dinucleotide (FADH2) electron transporters are synthesized and further utilized by respiratory chain complexes that are localized in the inner mitochondrial membrane (Moindjie et al., 2021; Read et al., 2021) The mitochondria's ability to use various carbon sources present in the cell microenvironment explains why they can switch from one metabolic pathway to another. Because of this adaptive characteristic, mitochondria are the key to metabolic flexibility, a crucial process for both carcinogenesis and cellular homeostasis (Moindjie et al., 2021). Nonetheless, the central question still remains about how the activation of cellular oncogenes controls the metabolic rewiring of the cells.

1.2.2 Electron transport chain and mutation in KRAS gene: a crosstalk between KRAS and mitochondria

KRAS signaling provides the building blocks required for cell growth and supports cellular bioenergetic demands by coordinating many metabolic pathways, such as the lipid, nucleotide, and glycolytic pathways. According to Hu et al. (2012) and Vafa et al. (2002), some proteins, including c-myelocytomatosis oncogene product (c-MYC), and hypoxia-inducible factor 1 alpha (HIF-1α) may also contribute to Warburg effect. These downstream proteins of the PI3K/AKT and MAPK pathways, respectively, may be crucial in increasing glycolysis rate and may also be involved in "metabolic reprogramming" in cancer cells (Muyinda et al., 2021; Kikuchi et al., 2016). Transcription factors HIF-1α and HIF-2α are associated with cancer development via intratumoral hypoxia and growth factor signaling induction. The amount of oxygen has a significant impact on HIF-1α activity. Post-translational modifications have a regulating role in its interaction with many tumor suppressor genes, including arrest-defective-1 protein (ARD-1), p300/CBP, and von Hippel-Lindau (pVHL). HIF-1α binds to pVHL under normal oxygen levels, resulting in pVHL-mediated ubiquitination and quick proteasome destruction. On the other hand, HIF-1α is stabilized in hypoxic conditions, accumulates, translocates to the nucleus, dimerizes with HIF-1β, and interacts with the co-activator p300/CBP to modulate the transcription of numerous hypoxia-inducible target genes, particularly those involved in angiogenesis, cell proliferation, survival, and metabolism (Muyinda et al., 2021; Chun et al., 2010).

Chun et al. identified a number of genes involved in mitochondrial phospholipid synthesis, including phosphoenolpyruvate carboxykinase 2 (PCK2), lysophosphatidylcholine acyltransferase 4 (LPCAT4), and acyl CoA synthetase 5 (ACSL5) controlled by both KRAS and HIF-1α. Cardiolipin, a component of the inner mitochondrial membrane, is involved in respiration through its interactions with electron transport chain proteins (Chun et al., 2010).

One of the main energy sources for the synthesis of ATP inside the mitochondria is the respiratory chain of the mitochondria. This mechanism involves two electron carriers, ubiquinone and cytochrome c, as well as five complexes. ATP synthase (Complex V) produces ATP via two pathways: I-III-IV and II-III-IV, which are powered by the electron gradient created by complexes I–IV (Zhao et al., 2019).

A mutation in the KRAS proto-oncogene often results in increased generation of reactive oxygen species (ROS) and inhibition of respiration. Cancer cells continue to produce the necessary amounts of ROS to keep up the mutagenesis process (Hu et al., 2012; Schieber &

Chandel, 2014). Since mitochondria are the primary location of ROS production, it is conceivable that inhibiting the electron transport chain will cause cancer by promoting mitogenic pathways by maintaining consistently elevated superoxide formation and by shifting metabolic pathways towards glycolysis (Neuzil et al., 2012; Schieber & Chandel, 2014). According to Zhao et al., there are many locations in the electron transport chain where electron leakage can result in the production of ROS. These locations include IF and IQ sites in complex I, site IIF in complex II, and site IIIQo in complex III (Fig. 3). For this reason, this complex could be a possible target for the mutant KRAS.

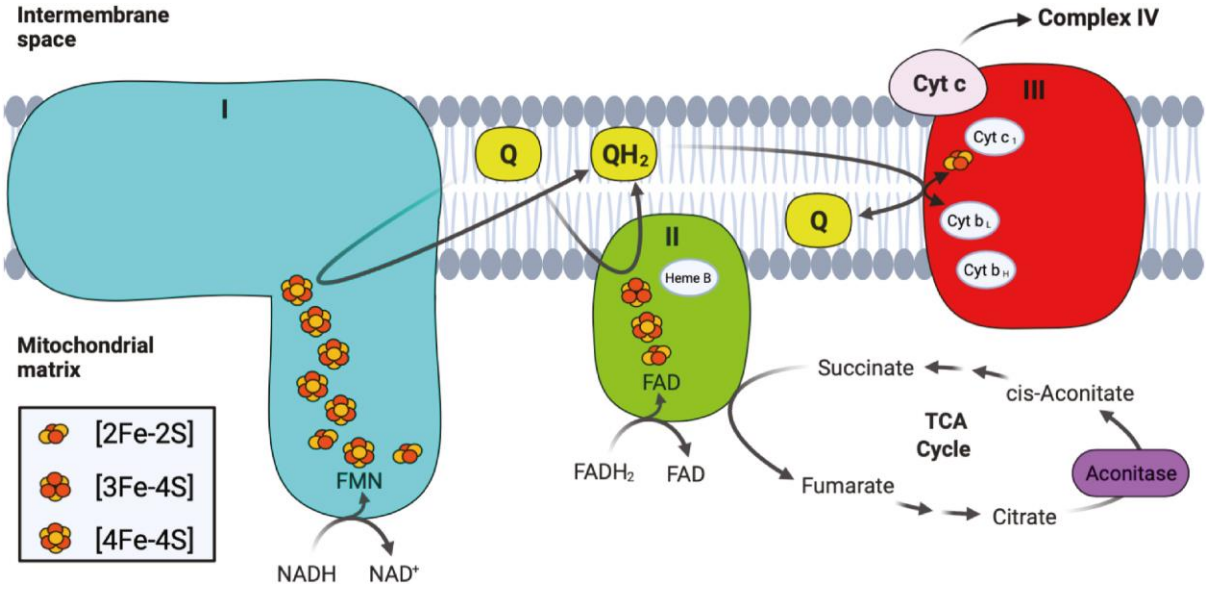

Figure 3. *Simplified version of the mitochondrial ETC (Read et al., 2021)*

Both directly interacting with the mitochondrial membrane and indirectly through signaling cascades are two ways that mutant KRAS protein might disrupt mitochondrial function. Numerous studies have previously demonstrated that mutant KRAS can obstruct respiration by translocating and accumulating the mutant protein on the mitochondria's outer membrane (Hu et al., 2012; Bivona et al., 2006). According to Hu and colleges' research, 60% of the KRAS protein was localized inside the mitochondria, whereas less than half was discovered on the mitochondrial membrane (Hu et al., 2012).

As a previous study showed the translocation of the KRAS protein onto the outer membrane of the mitochondria may play an important role in mediating metabolic rewiring towards aerobic glycolysis in cancer cells. Even though the exact role of such translocation in suppressing mitochondrial respiration remains unclear, the study suggests that the KRAS protein localizes on mitochondria, contributing to the inhibition of the respiratory chain by deregulation of NADH dehydrogenase activity. This finding highlights the importance of the

mitochondrial electron transport chain regulation in metabolic switch mediated by mutations in the KRAS gene (Hu et al,.2012).

1.3 ATO/D-VC – a new hope for KRAS- mutant cancer treatment

1.3.1 What is ATO/D-VC and how does it work?

Mutation in KRAS proto-oncogene is responsible for 25-30% of the global number of cancers. It is the most frequent genetic alteration of pancreatic ductal adenocarcinoma with up to 95% of KRAS-mutant cancers (Luo, 2021; Wang et al., 2013). On top of it, the mutation in the KRAS gene is associated with poor therapeutic prognosis and several challenges not only in treatment but in resistance to several already developed drugs (Luo, 2021).

The combination of arsenic trioxide and D-vitamin C is a relatively new approach to targeting KRAS mutant cancer through the cytotoxic production of reactive oxygen species. In previous studies, it was demonstrated that ATO/D-VC leads to apoptosis in AK192 pancreatic cancer cells which is associated with the excessive production of superoxide (Begimbetova et al., 2022). Several studies provided the data that highlights the efficiency of the ATO/D-VC drug combination both in colorectal and pancreatic cell lines and xenografted mouse model. Even though L-vitamin C (L-VC) and its enantiomer, D-vitamin C (D-VC), showed quite similar results in combination with ATO in cultured cells, the mouse model solidly proved that arsenic trioxide in combination with D-vitamin C is more effective than with its L form. That can be explained by the fast oxidation of L-VC to dehydroascorbate (DHA). This reaction is chirality-dependent and occurs with 8 times slower rates for D-VC and as a result, leads to its accumulation in the bloodstream of the mice and higher uptake by cancer cells (Wu et al., 2020).

Recent study showed that the potency of D-VC in generating ROS in cultured cell is similar to L-VC, however, the authors questioned the toxicity of both enantiomers on mice. Begimbetova et al. demonstrated that a high dose of 9.2 g/kg of L-VC was more toxic in comparison to D-VC that was shown by the drop in mice survival. Over the study period, D-VC showed a slight 20% decrease in percentage of mice survived whereas L-VC was lethal on the day 18. This can be explained by the overall health conditions of the mice subjected to the treatment with L-VC. The mice appeared unwell, had a reduced appetite and partial hair loss. They also developed ulcers on their back and pelvis that were associated with

inflammation. In contrast, the mice injected with D-VC did not display these symptoms. This research demonstrated the safety reason for utilizing D-VC instead of its natural L-VC form for the further clinical studies (Begimbetova et al., 2024).

Still, the exact mechanism behind suicidal ROS production remains unknown and there is still a wide range for the investigation.

1.3.2 Proposed mechanism of action of ATO/D-VC drug combination.

One possible explanation for the synergetic effect of the drugs was proposed by Burska et al. KRAS-mutant cells are superior to normal cells in terms of the level of glucose consumption which can be explained by the well-known Warburg effect. High glucose uptake is mediated by overexpressed GLUT1 transporter which is the advantage and one of the weak points of cancer cells at the same time (Kaźmierczak-Barańska et al., 2020; Ngo et al.,2019). D-vitamin C can enter the cell through the GLUT1 transporter in the form of dehydroascorbate (DHA) and further be converted back into D-VC at cost of the glutathione (GSH) oxidation. Constant depletion of the GSH pool can trigger oxidative stress that is associated with ROS accumulation and glyceraldehyde 3-phosphate dehydrogenase inactivation. It subsequently activates the apoptotic pathways and induces cell death in highly glycolytic KRAS-mutant cancer cells (Burska et al., 2022; Yu et al., 2023)

Arsenic trioxide (ATO) being uptaken by the cell can be neutralized by GSH, methylated, and subsequently eliminated from the cell. However, if the total GSH pool is already affected by D-VC, ATO can act directly on thiol reactive groups on cysteine residues of the mitochondrial proteins that are the parts of the respiratory chain. Such an effect of ATO induces improper coordination of Fe-S clusters that are essential for electron transport within each complex (Burska et al., 2022). In addition to this, Vitamin C is as well a potent reducing agent for iron residues (Yu et al., 2023).

In combination, it results in the impairment of functionality of the proteins of the electron transport chain that elevates the amount of ROS production to the cytotoxic level. However, the question that needs to be addressed is which complex is truly affected by ATO/D-VC treatment.

In mitochondria, there are two major sites of ROS production. Complex I is considered to be the main respiratory chain complex that can generate ROS in mitochondria. Eight of 12 total Fe-S clusters are found to be a part of this complex starting from its NADH binding site and ending at the site of ubiquinone binding. ROS can be produced from both these ends of the Fe-S cluster chain. Hence, blockage of the quinone binding site by complex I -specific

inhibitor rotenone leads to the overproduction of flavin mononucleotide (FMNH) causing electron leakage (Read et al., 2021; Kowaltowski et al., 2009; Chen et al., 2003).

Another key ROS generator in mitochondria is Complex III. The site of ubiquinone oxidation is responsible for ROS production which was shown by antimycin A inhibition of quinone reductase site by blocking the electron transfer and increasing the lifetime of semiubiquinone. Semiubiquinone can react afterward with O_2 to form superoxide (Kowaltowski et al., 2009; Chen et al., 2003).

Both complexes I and III can be a potential target of the ATO/D-VC drug combination. It is possible that ATO/D-VC downregulates the activity of these complexes leading to SRPM followed by apoptosis. In addition to it, the possible involvement of complex II cannot be excluded as it also believes to a site of ROS production through flavin part of the molecule as was previously described (Fig.4).

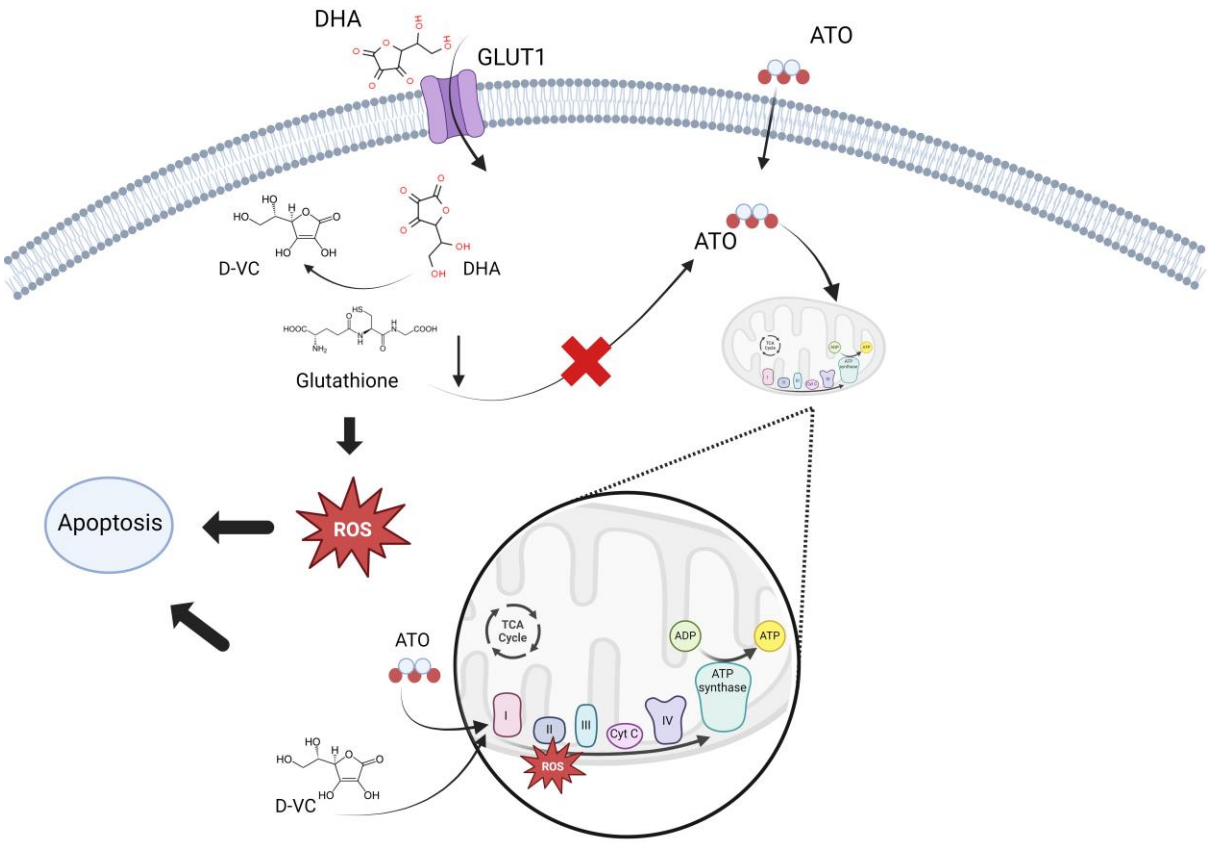

Figure 4. *Proposed mechanism of action of ATO/D-VC in KRAS-mutant cancer cells. (The graph was created using BioRender.com)*

2 MATERIAL AND METHODS

2.1 Tissue culture and ATO/D-VC treatment

Two cell lines are utilized for the current research: AK192 mouse pancreatic adenocarcinoma cell line with doxycycline-inducible KRAS ($KRAS^{G12D}$) expression that was kindly provided by Drs. Haoqiang Ying and HCT116 ($KRAS^{G13D}$) obtained from human colorectal cancer.
The cells were plated in Dulbecco's modified Eagle's medium supplemented F-12 with 10% fetal bovine serum, 2 mM L-glutamine, Penicillin G sodium salt, and Streptomycin sulfate salt.
For flow cytometry analysis, AK192 cells were seeded on 6-well plates with the seeding density 150,000 cells per well with 2 g/L of doxycycline added to the media and HCT116 were plated at 400,000 cell per well.
For enzymatic activity assay, AK192 were seeded on 150mm coated tissue culture plates at densities 3,000,000 in 20 ml cell culture medium with the addition of doxycycline (2 g/L). HCT116 were cultured at the initial seeding density of 6,000,000 cells in 20ml of DMEM F-12. Cells are treated with 5μM ATO and 1mM D-VC for AK192 and 7.5μM ATO and 1.5mM D-VC for HCT 116 24 at hours post-seeding.

2.2 Flow cytometry analysis of cell death and superoxide production.

The seeding and treatment conditions were as described above. Propidium iodide (PI), Annexin V and MitoSOX staining were performed as described in Begimbetova et al. (2022) using Attune NxT Flow Cytometer.
The preparations of the samples were performed as follows:

1. The media was collected to the 15 ml tube;
2. The cells were washed in 1 ml of PBS and collected as well to the same tube;
3. 300 μl of 1x trypsin was added to the plate and incubated for 5 minutes;
4. 700 μl of DMEM F-12 media were added and the cells were collected to the same 15 ml tube;
5. The cells were counted using MultiSizer (Beckman) and 500,000 cells per condition were used for further staining;

6. Samples were centrifuged at 300 g for 5 minutes at room temperature and washed with 1ml of PBS;
7. The washing step was repeated, and PBS was discarded;
8. The staining was performed at the final concentration of PI of 100µg/µl and 5µl of Annexin V. MitoSOX staining was performed in the media without serum for 30 minutes at 37^{o}C in the dark at the final concentration of 2.5µM.
9. For each assay at least 30,000 events were acquired.

2.3 Mitochondria isolation

Mitochondria isolation from cultured cells was performed according to the protocol described in Spinazzi et al. (2012) with the adjustment of the volumes. In brief, the culture medium was removed, and the cells were washed once with ice-cold PBS. The cells were scraped in 1 mL of ice-cold PBS, and cell suspension was transferred to 1.5 ml Eppendorf tubes. The cells were washed by centrifugation at 1,000g for 5 min at 4 °C, and the supernatant was discarded. The cells were then resuspended in 1 ml of ice-cold PBS and subjected to another round of washing. After centrifugation, the supernatant was discarded, and cells were suspended in 1 ml of 10 mM ice-cold hypotonic Tris buffer (pH 7.6). Homogenization was performed using pre-cooled glass/Teflon tissue grinder with 25 slow up-down strokes. To the cell homogenate, 200 µl of 1.5 M sucrose solution was added and thoroughly mixed. The mixture was then centrifuged at 600g for 10 min at 4°C, and the resulting supernatant was collected and further centrifuged at 14,000g for 10 min at 4 °C. The supernatant was carefully discarded, and the mitochondrial pellet was resuspended in 10 mM ice-cold hypotonic Tris buffer (pH 7.6). The mitochondrial solution was divided into several aliquots and stored at -80 °C. Isolated mitochondria were used to perform complex I enzymatic activity assay. The frozen mitochondrial solution was subjected to three cycles of freeze-thawing in liquid nitrogen to disrupt the mitochondrial membranes. Total protein content was measured according to the Bradford method (Spinazzi et al., 2012).

2.4 Cell lysate preparation

Total cell lysate was prepared according to Spinazzi protocol with several modifications. Cells were washed once with ice-cold PBS after removing them from the medium. Cells were scraped in 1 mL of ice-cold PBS and collected to 1.5 mL Eppendorf tubes. The cells were washed twice by centrifugation at 1,000g for 5 min at 4 °C and resuspended in 1 ml of PBS. After the second round of centrifugation and removal of the supernatant, the cell pellet was stored in aliquots at -80 °C. Before respiratory chain enzymatic activities measurements cells were diluted in 20mM hypotonic potassium phosphate buffer (pH 7.5) and snap-frozen in liquid nitrogen and thawed at 37 °C three times. Total protein content was measured according to the Bradford method (Spinazzi et al., 2012). Total cell lysates were used for complex II, III and IV activity assay at the specific for each complex amount of proteins loaded per reaction.

2.5 Mitochondrial electron transport chain enzymatic activity

The assay for mitochondrial respiratory chain enzymatic activities assessment was conducted according to Spinazzi protocol except complex I activity assay. In complex IV enzymatic activity assay n-Dodecyl-β-D-maltoside was added to the reaction as suggested by Birch-Machin & Turnbull (2001). All spectrophotometric measurements were performed in 1 ml cuvette at 37^{o}C using NanoDrop 2000c Spectrophotometer (Thermo Scientific) (Spinazzi et al., 2012) (Table 1).

Table 1. Summary of conditions for spectrophotometric assays.

	Complex I	**Complex II**	**Complex III**	**Complex IV**
λ (nm)	340	600	550	550
ε (mmol−1 cm−1)	6.2	19.1	18.5	18.5
Buffer	Tris-HCl, 20mM	KP, 25 mM	KP, 25 mM	KP, 50 mM
pH	7.5	7.5	7.5	7.0
Substrates/ electron acceptors	NADH, 120 µM	Succinate, 20 mM DCPIP, 80 µM DUB, 50 µM	DubH2, 100 µM Cyt c, 75 µM	Cyt c H2, 60 µM
Detergent			Tween-20 (0.025% (vol/vol))	
Specific Inhibitor	Rotenone 25 µM	Malonate, 10 mM	Antimycin A, 10 µg ml − 1	KCN, 300 µM

Complex I (NADH:ubiquinone oxidoreductase) is assessed using a spectrophotometric method by measuring the decrease in NADH absorbance at 340 nm. Mitochondrial membranes are added to a 500 µl reaction solution containing 20 mM Tris-HCl pH 7.5, 2 mg/ml fatty acid-free BSA, and 20 µM horse-heart cytochrome c. The reaction starts with the addition of 500 µl of 240 µM NADH in 20 mM Tris-HCl pH 7.5, and the mixture is quickly vortexed before being transferred to a cuvette to monitor the absorbance changes for 3 minutes. The final concentrations are 120 µM NADH, 1 mg/ml fatty acid-free BSA, and 10 µM horse-heart cytochrome c. The mitochondrial membrane concentration is 20 µg protein/ml. To account for background activities from other NADH-oxidizing enzymes, inhibitor-insensitive activity is measured using 25 µM rotenone and then subtracted. Complex I inhibition is measured by adding it post-recording NADH oxidase activity, and absorbance changes are observed for an additional 3 minutes. (Salscheider et al., 2022) (Table 2).

Table 2. The purpose of each regent utilized in Complex I assay.

Reagent	**Purpose**
NADH (Nicotinamide adenine dinucleotide)	*Substrate for complex I activity*
Tris-HCl buffer (pH 7.5)	*Maintains the pH of the reaction mixture at a constant value of 7.5*
Fatty acid-free BSA (Bovine Serum Albumin)	*Protein stabilizing agent*
Horse-heart cytochrome c	*Electron carrier*
Rotenone	*Complex I specific inhibitor*

Complex II (succinate dehydrogenase) assay involves a buffer containing 600 µl of distilled water, 50 µl of 0.5 M potassium phosphate buffer (pH 7.5), 20 µl of 50 mg/ml fatty acid-free BSA, 30 µl of 10 mM KCN, 50 µl of 400 mM succinate, 70 µg of total cell lysate, and 145 µl of 0.015% (wt/vol) DCPIP. The volume is adjusted to 996 µl with distilled water. The cuvette is mixed, incubated at 37°C for 10 minutes in a spectrophotometer, and the baseline is read at 600 nm for 3 minutes. The reaction starts with the addition of 4 µl of 12.5 mM DUB, and the decrease in absorbance at 600 nm is tracked for 3 minutes. Specificity of complex II activity is verified by adding 10 µl of 1 M malonate before starting the reaction (Spinazzi et al., 2012) (Table 3).

Table 3. The purpose of each regent utilized in Complex II assay.

Reagent	**Purpose**
Succinate	*Substrate for complex II activity, serves as the electron donor*
Potassium phosphate buffer (pH 7.5)	*Maintains the pH of the reaction mixture at a constant value of 7.5*
Fatty acid-free BSA (Bovine Serum Albumin)	*Protein stabilizing agent*
DCPIP (2,6-dichlorophenolindophenol)	*Serves as an electron acceptor*
KCN (Potassium cyanide)	*Specific inhibitor of Complex IV (cytochrome c oxidase), increases the specificity of the assay by eliminating all the activity related to Complex IV*
DUB (decylubiquinone)	*An artificial electron acceptor that mimics the role of ubiquinone*
Malonate	*Complex II specific inhibitor*

For the measurement of ***Complex III (decylubiquinol cytochrome c oxidoreductase)*** reaction mix included 730 µl of distilled water, 50 µl of potassium phosphate buffer (0.5 M, pH 7.5), 75 µl of oxidized cytochrome c, 50 µl of KCN (10 mM), 20 µl of EDTA (5mM, pH 7.5), 10 µl of Tween-20 (2.5% (vol/vol)) and 20 µg of cell lysate. In parallel, a separate cuvette was prepared with the same reagents and sample, but with the addition of 10 µl of 1 mg ml−1 antimycin A solution. Both cuvettes were adjusted to a volume of 990 µl with distilled water. The baseline was read at 550 nm for 2 minutes. The reaction was initiated by adding 10 µl of 10 mM decylubiquinol. The cuvettes were rapidly mixed by inverting them using Parafilm, and the increase in absorbance at 550 nm was immediately observed for 2 minutes. The specific activity of Complex III is the antimycin A-sensitive activity (Spinazzi et al., 2012) (Table 4).

Table 4. The purpose of each regent utilized in Complex III assay.

Reagent	**Purpose**
Oxidized cytochrome c	*Mobile electron carrier*
Potassium phosphate buffer (pH 7.5)	*Maintains the pH of the reaction mixture at a constant value of 7.5*
EDTA (Ethylenediaminetetraacetic acid, pH 7.5)	*Chelating agent that binds divalent metal ions such as magnesium and calcium. Prevents metal ion-dependent interference in the assay*
Tween-20	*Non-ionic detergent that helps in solubilizing hydrophobic molecules*
KCN (Potassium cyanide)	*Specific inhibitor of Complex IV (cytochrome c oxidase), increases the specificity of the assay by eliminating all the activity related to Complex IV*
Decylubiquinol	*Electron donor that mimics the reduced form of ubiquinone*
Antimycin A	*Complex III specific inhibitor*

For the measurement of ***Complex IV (cytochrome c oxidase)*** activity, the following steps were performed: In a 1-ml cuvette, 400 µl of distilled water, 250 µl potassium phosphate buffer (100 mM, pH 7.0), 15 µl n-Dodecyl-β-D-maltoside (30mM) and 50 µl reduced cytochrome c (1 mM) were added, and the baseline activity was recorded at 550 nm for the last 2 minutes. The volume was adjusted to 995 µl with distilled water. The reaction was

initiated by adding 30 µg of total cell lysate. The mixture was inverted to mix the contents, and the decrease in absorbance at 550 nm was monitored for 3 minutes (Spinazzi et al., 2012; Birch-Machin & Turnbull, 2001) (Table 5).

Table 5. The purpose of each regent utilized in Complex IV assay.

Reagent	**Purpose**
Reduced cytochrome c	*Mobile electron carrier*
Potassium phosphate buffer (pH 7.0)	*Maintains the pH of the reaction mixture at a constant value of 7.0*
n-Dodecyl-β-D-maltoside	*Confer the conformation of the enzyme in an active state*
KCN (Potassium cyanide)	*Complex IV specific inhibitor*

The enzymatic activities were calculated as nmol min^{-1} mg^{-1} of protein according to the following equation:

Enzyme Activity = (∆Absorbance/min * 1000)/(extinction coefficient * volume of sample in mL * sample protein concentration in mg/mL)

2.6 Statistical analysis

Obtained data is analyzed by GraphPad Prism 8 with the application of appropriate statistical tests. Flow cytometry data is processed by FCS Express.
The whole workflow is illustrated in the Figure 5.

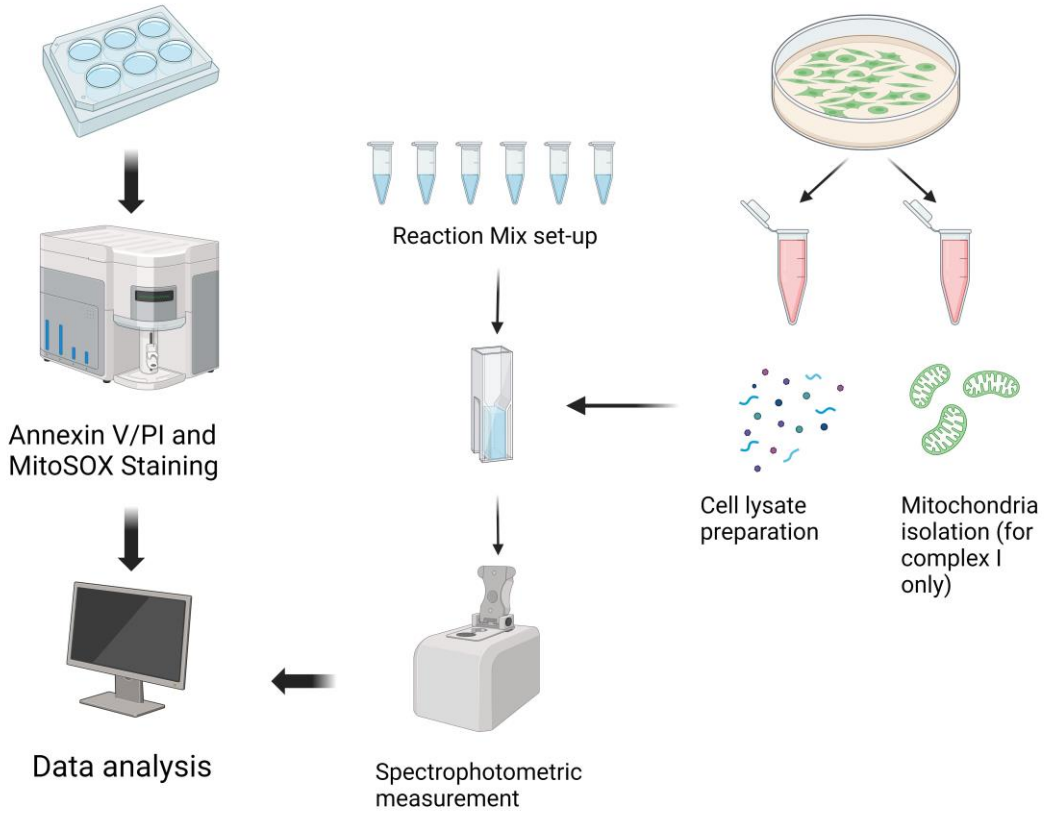

Figure 5. *The schematic workflow (The graph was created using BioRender.com).*

3 AIMS OF THE THESIS PROJECT

The **hypothesis** for the current research is that arsenic trioxide and D-Vitamin C drug combination induces cell death in KRAS-mutant cancer cells by suicidal ROS production through the alternation of electron transport chain activity.

To test the hypothesis several aims should be achieved:

Aim 1. Assessment of the effect of ATO/D-VC treatment on KRAS mutant cancer cells

Objectives:

- → To perform apoptotic assay in ATO/D-VC treated cells in comparison to untreated.
- → To assess the level of ROS production in ATO/D-VC treated KRAS-mutant cancer cells.

Aim 2. Evaluate the impact of ATO/D-VC treatment on the enzymatic activity of the complexes of the electron transport chain.

Objective:

- → To measure activities of ETC complexes in KRAS mutant cancer cell lines treated with ATO/D-VC

4 RESULTS

4.1 ATO/D-VC induces cytotoxic ROS production by mitochondria in HCT116 and AK192 with subsequent apoptosis.

From the bright field microscopy images morphological changes can be already observed at 24 hours post ATO/D-VC treatment in AK192 cell line in comparison to control (GM). At 48 hours a pronounced effect of ATO/D-VC drug combination can be detected with most of the cell detached from the plate (Fig. 6).

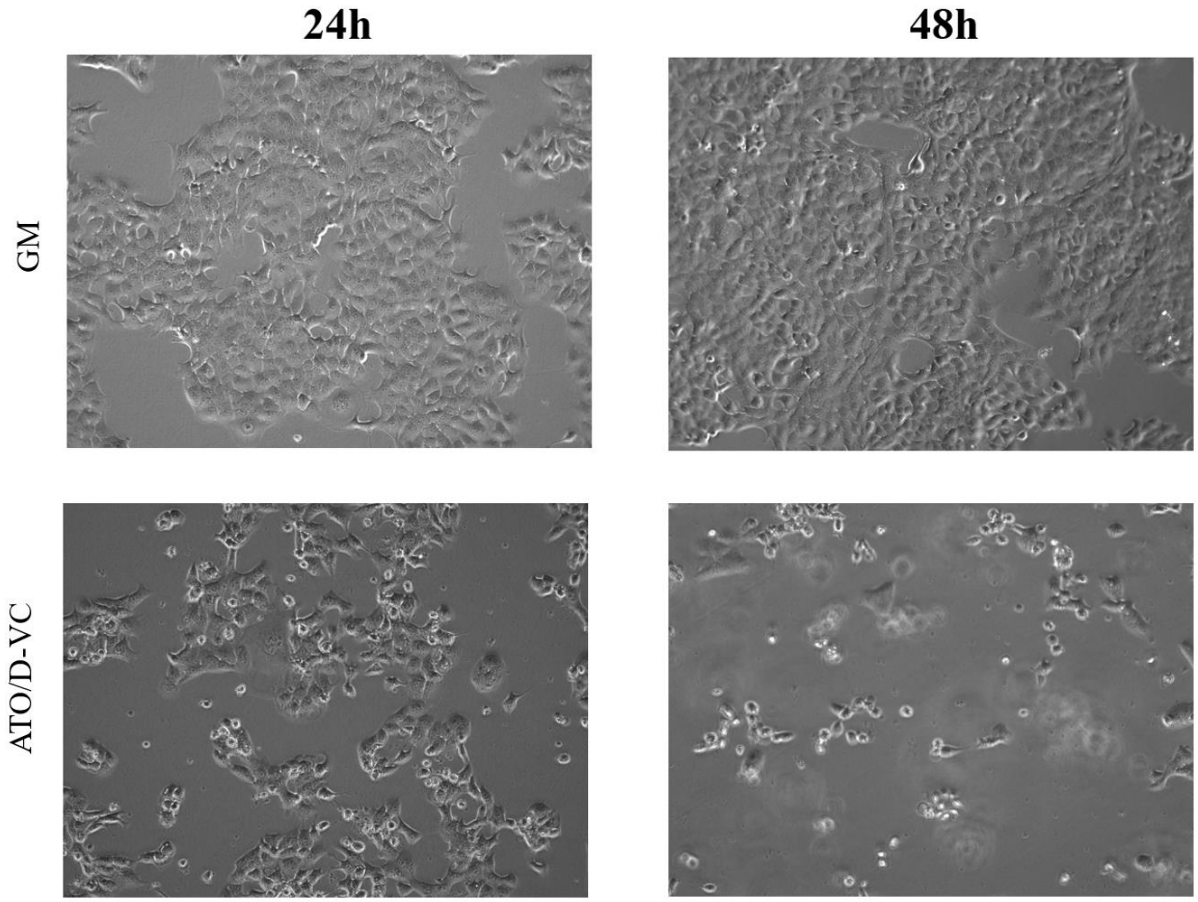

Figure 6. *Bright field images of AK192 cells under ATO/D-VC treatment.*

In HCT116 the effect was expected to be observed at 48 hours acording to Wu et al., 2020, however, ATO/D-VC showed little or no effect after 24 and 48 hours, regardless of ATO and D-VC concentrations, but a strong effect was observed at 72 hours (Fig. 7).

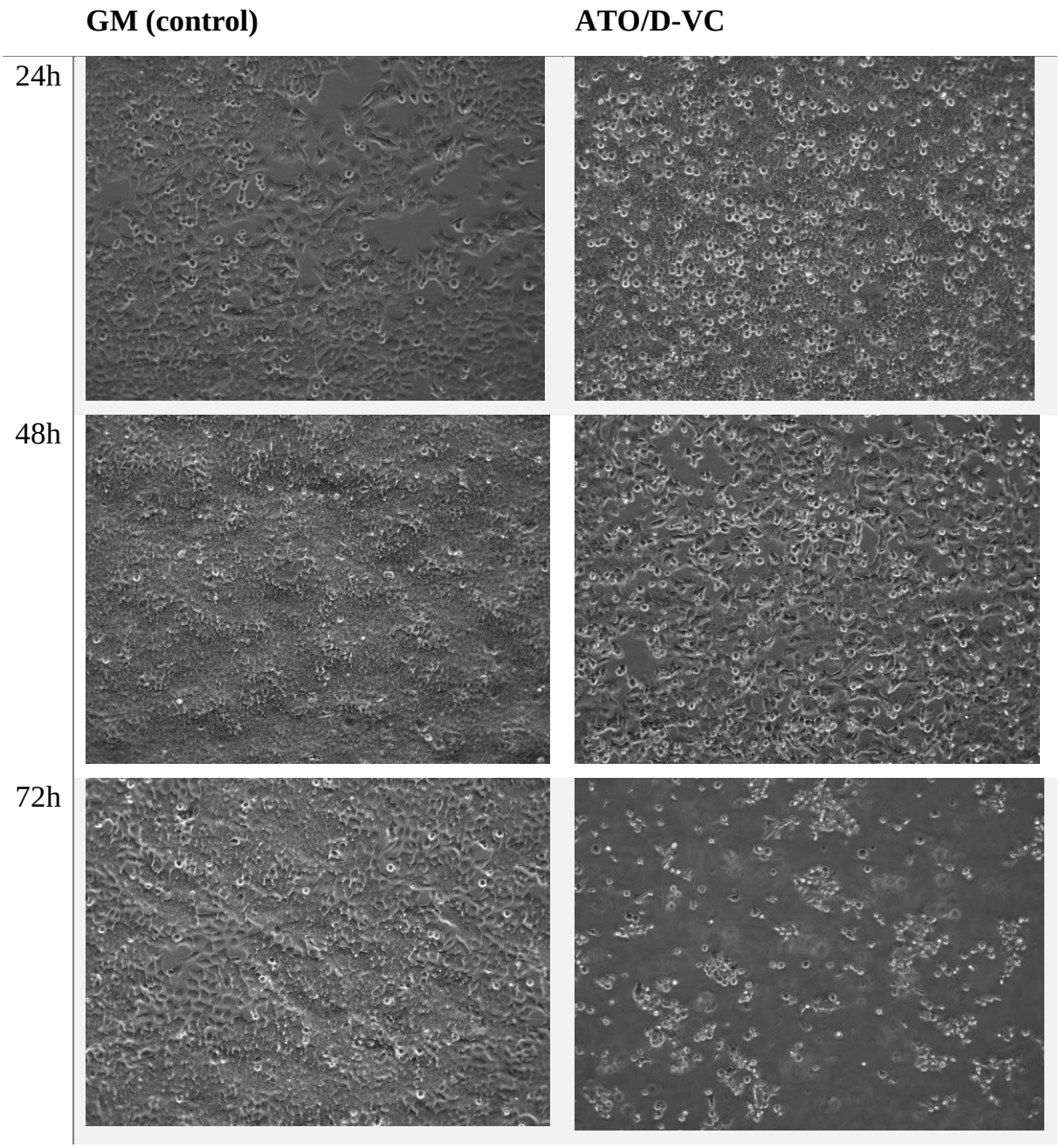

Figure 7. *Bright field images of HCT116 for ATO/D-VC treatment at 24, 48, 72 hours.*

Based on the observations on the bright field microsope it was decided to run viability assay on samples collected at 24 and 48 hours for both AK192 and HCT116 cell lines.

In AK 192 the percentage of late apoptotoic cells increased 2.8 and 2.3 times upon treatment for 24 and 48 hours respectively. HCT116 under ATO/D-VC treatment showed 1.6 and 6.2 fold increase in percentage of cells in late apoptotic stage (Fig. 8).

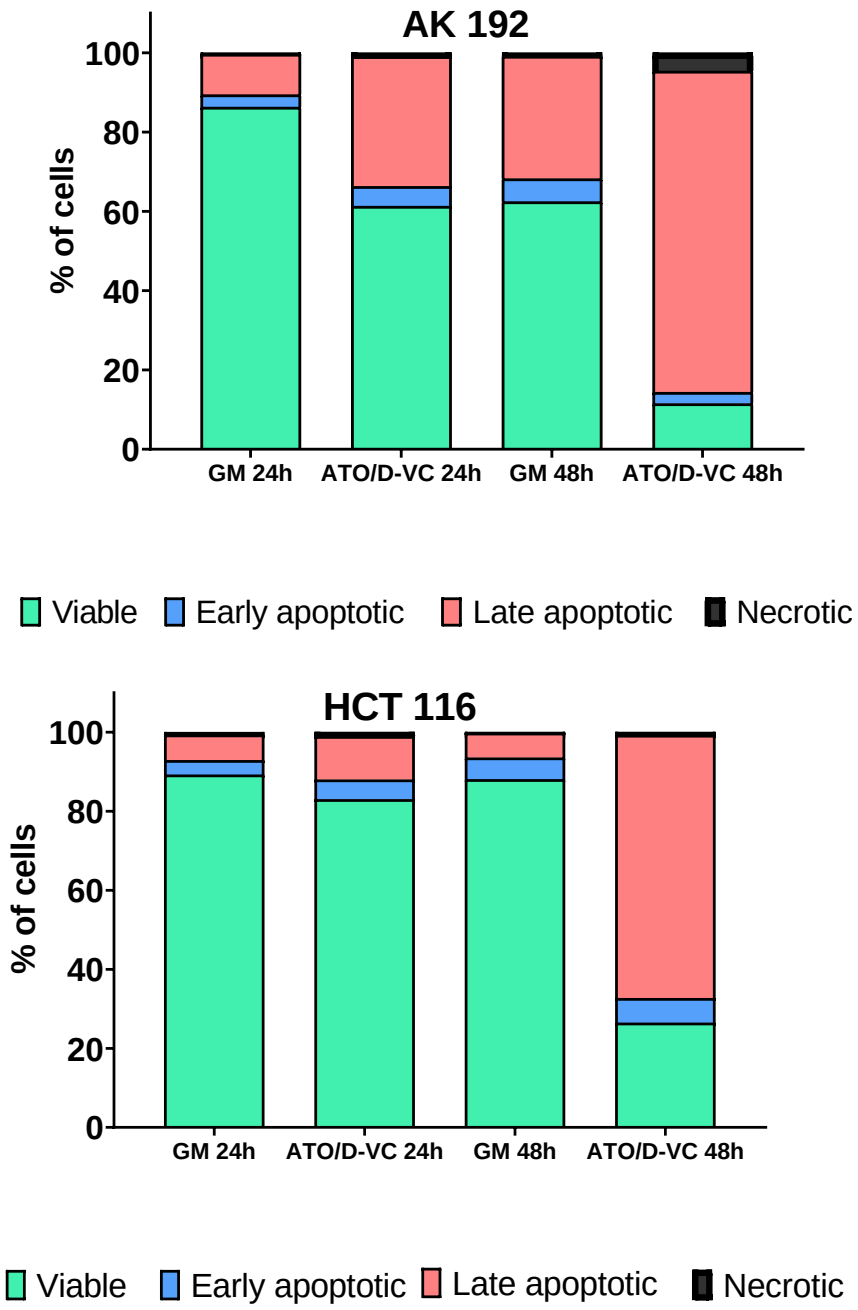

Figure 8. *Flow cytometric assessment of apoptosis in AK192 and HCT116 treated with ATO/D-VC combination. The results are presented in percentage.*

It was proposed that cell death is triggered under ATO/D-VC treatment due to suicidal ROS production by mitochondria. To indentify the level of ROS production MitoSOX staining was performed which indicates superoxide production by the cell.

The increase in mitochondrial ROS production can be detected under ATO/D-VC treatment with 7.7 and 6.8 fold difference in AK 192 and 2.6 and 12.8 fold in HCT 116 at 24 and 48 hours respectively (Fig. 9).

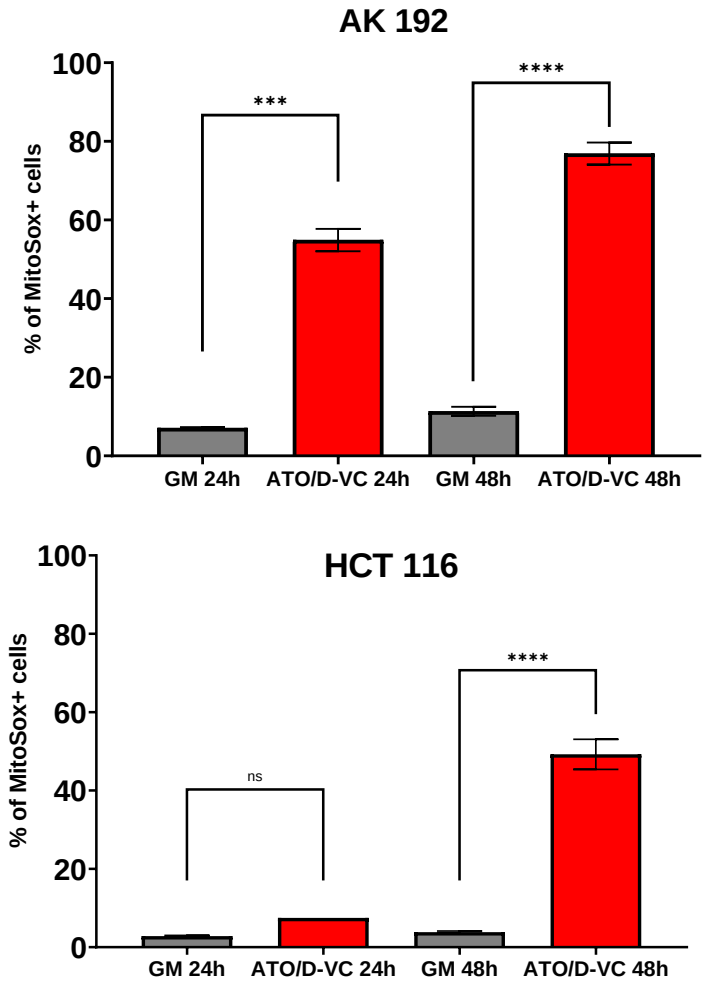

Figure 9. *Flow cytometry analysis of ROS production in AK192 and HCT116 cell lines upon ATO/D-VC drug combination. The results are presented as mean of three independent experiments (mean ± SD). * $p < 0.05$, *** $p < 0.001$, **** $p < 0.0001$.*

4.2 ATO/D-VC alters succinate dehydrogenase's activity in AK192 and HCT116 cell lines.

In AK192 ATO/D-VC treatment downregulates the activity of succinate dehydrogenase (Complex II), cytochrome c reductase (Complex III) and cytochrome c oxidase (Complex IV) with 2.3-, 2.4 and 1.1-fold change respectively. However, the activity of NADH dehydrogenase (Complex I) remained unaffected (Fig. 10).

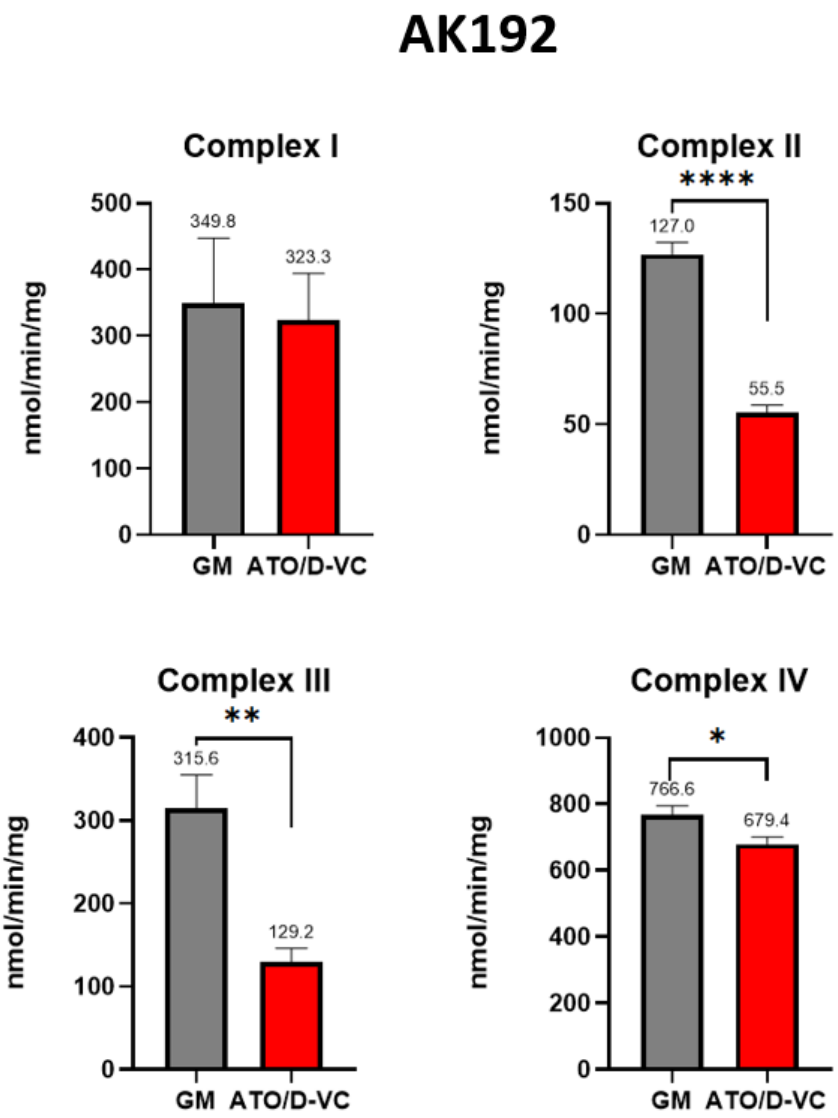

Figure 10. *Enzymatic activity of mitochondrial electron transport chain in AK192 cell line at 24 hours post ATO/D-VC treatment. The results are presented as mean of three independent experiments each in triplicate (mean ± SEM). * $p < 0.05$, *** $p < 0.001$, **** $p < 0.0001$.*

In HCT116 cell line the drop in activity of Complex II and Complex IV can be observed at 48 hours with 1.3- and 1.2-fold change. However, in contradiction to AK192 Complex III activity remained unchanged (Fig. 11).

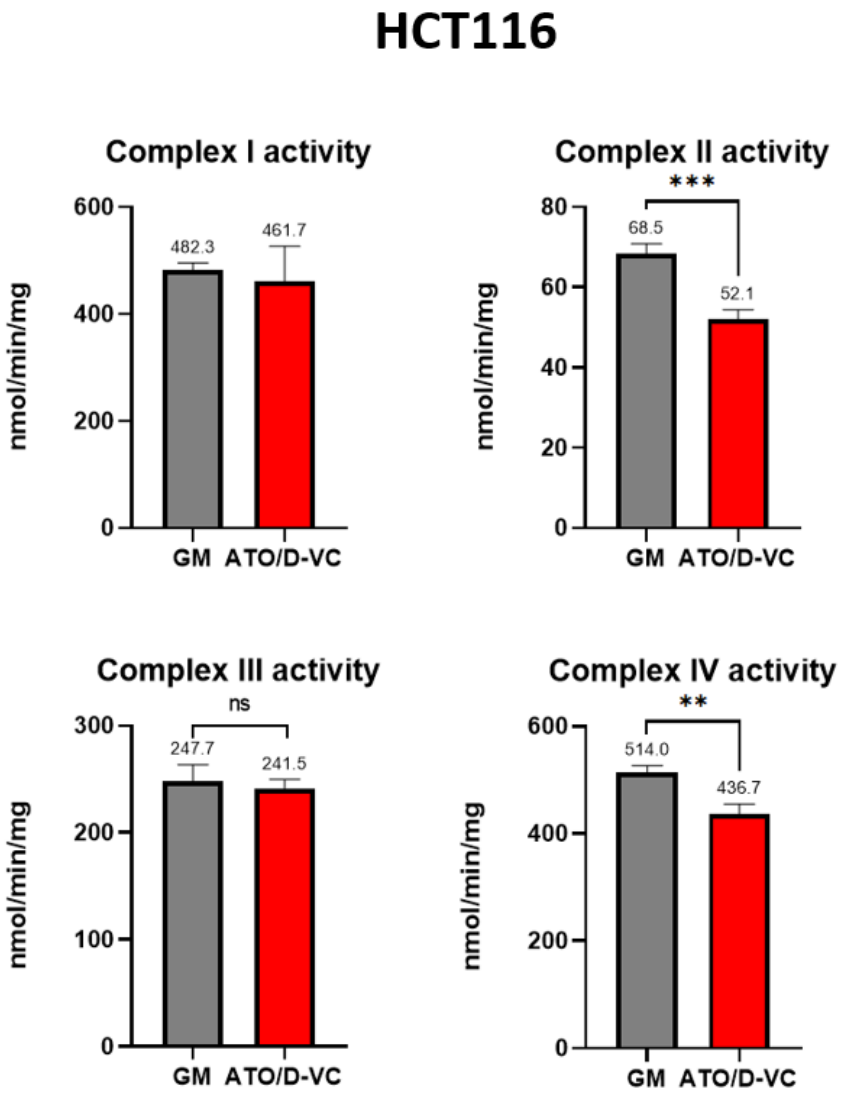

Figure 11. *Enzymatic activity of mitochondrial electron transport chain in HCT116 cell line at 48 hours post ATO/D-VC treatment. The results are presented as mean of three independent experiments each in triplicate (mean ± SEM). * $p < 0.05$, *** $p < 0.001$, **** $p < 0.0001$.*

4.3 Complex II inhibitor, 2-Thenoyltrifluoroacetone, protects cell from ATO/D-VC effect.

As it was previously shown, ATO/D-VC decreases the activity of Complex II of electron transport chain in both cell lines, however, it was believed for a long period of time that succinate dehydrogenase is not one of the ROS producing sites as it cannot leak the electrons as proton pumps such as Complex I and III do. Still, it was clearly stated that depending on inhibition site it still can produce ROS from dicarboxylate-binding site of the complex

(Zheng et al., 2024; Zhao et al., 2019; Read et al., 2021). For this reason, the preblockage of complex II was expected to give a partial rescue effect from ATO/D-VC treatment.

In this part of the experiment cells were preincubated for 1 hour with complex II inhibitor 2-Thenoyltrifluoroacetone (TTFA) followed by ATO/D-VC treatment and monitored for 24 and 48 hours. Even though no changes were observed at 24 hours in AK192 cell line, it can be seen that around 60% of the cells were still attached under ATO/D-VC treatment with pretreatment with TTFA at 48 hours (Fig. 12).

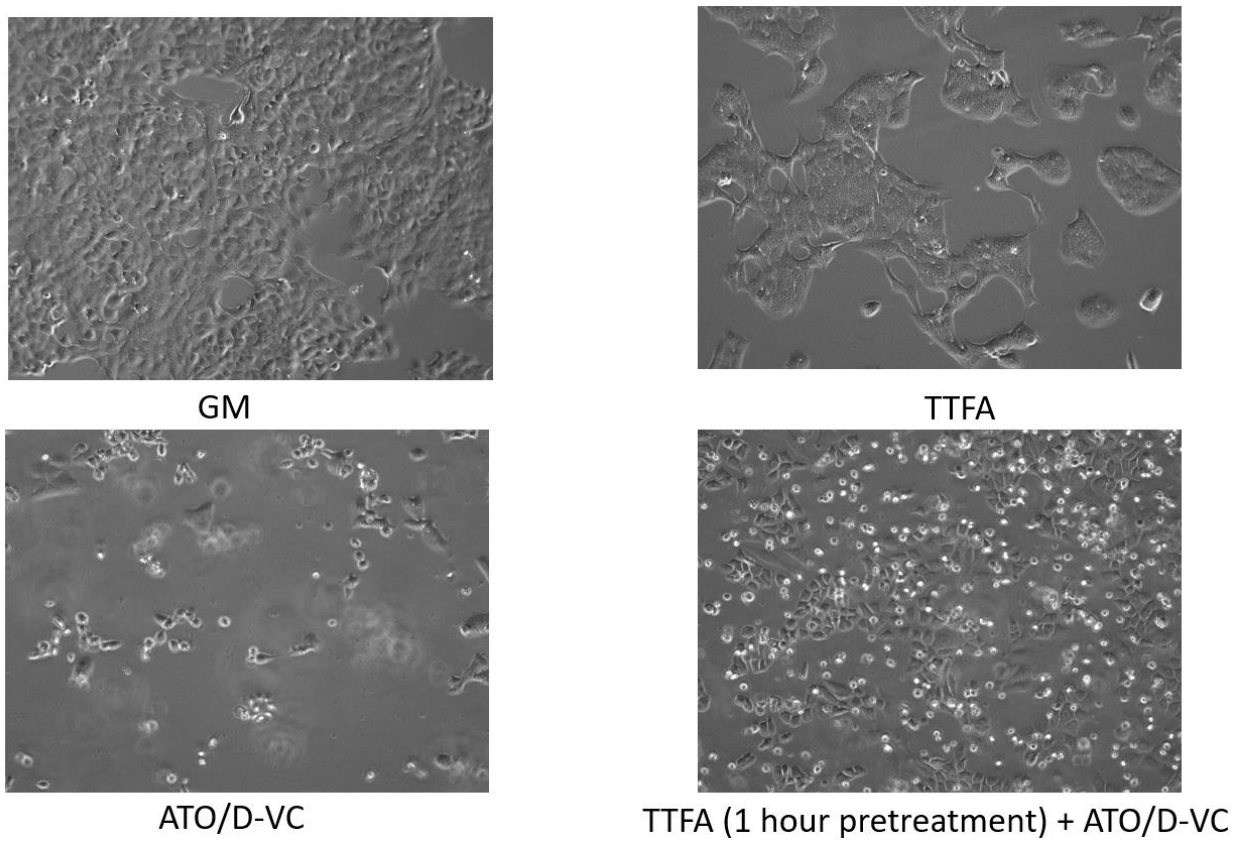

Figure 12*. Protective effect of complex II inhibitor TTFA in AK192 at 48 hours post ATO/D-VC treatment.*

5 DISCUSSION

As the current study showed, high level of ROS, superoxide in particular, produced under ATO/D-VC can be linked to the programmed cell death e.g. apoptosis which was observed in both cell lines. MitoSOX staining allows to detect superoxide formed by mitochondria showing that the primary site of ROS production lies within mitochondria itself. As it was described above three mitochondrial complexes of the electron transport chain are the ROS producing parts: complex I, complex II and complex III. The measurement of each complex enzymatic activity reviled the decrease in Complex II and complex IV activity in both cell lines and complex III in AK192 cell line. From this it can be deduced that complex II could be the target of ATO/D-VC and this subsequently leads to the drop in complex III and IV activity as the electron flow goes from II-III-IV. Complex I activity is probably insufficient to compensate for complex II downregulation which causes the decrease in complex III activity regardless of the possible flow from I-III-IV.

Moreover, this finding can be supported by available data which highlights that another arsenic compound, sodium arsenite, alters succinate dehydrogenase activity. Mitochondria exposed to several doses of sodium arsenite (25, 50, and 100 μM) showed a decrease in the conversion of MTT to formazan by the mitochondria (Fig. 13). However, after adding As (III), Cytochrome-c oxidase activity (Complex IV) remains unaffected (Hosseini et al., 2013).

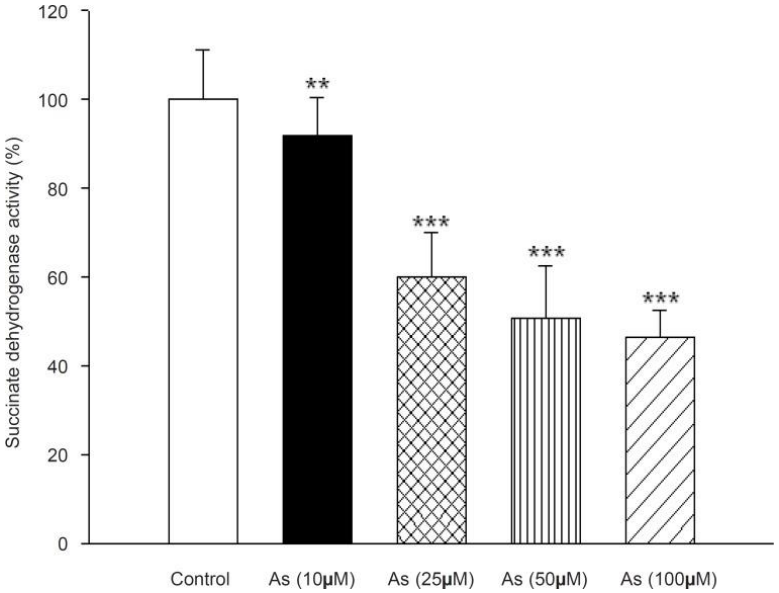

Figure 13. *Effect of arsenic on Succinate dehydrogenase (complex II) activity (Hosseini et al., 2013).*

The fact that complex II can be a main target of ATO/D-VC drug combination is supported by partial protection by Complex II preblockage with its inhibitor TTFA. Although it was believed that respiratory Complex I and Complex III were the primary sources of ROS, previous research has shown that Complex II also plays a significant role.

Current study shed some light on the molecular aspects of ATO/D-VC mechanism of action, however, further studies are required to get the more comprehensive view. Even though flow cytometry data suggests that cells die via apoptosis under treatment, it is worth testing whether they undergo the canonical apoptotic path or ferroptosis. Further experiments that can be done are western blot analysis of caspase-3 vs cleaved caspase-3 and cytochrome c release as well as apoptotic array which includes pro-apoptotic Bax, Bid, and BAD and anti-apoptotic Bcl-xL and Bcl-2 proteins of the Bcl-2 family as it was shown by Chen and colleagues that vitamin C leads to the release of cytochrome c and activation of apoptotic proteins caspase-9 and caspase-3. It also increased the Bax/Bcl-2 ratio, promoting apoptosis via the mitochondria-dependent pathway (Chen et al., 2019). It might be that D-VC in combination with ATO also triggers mitochondria-dependent apoptosis. Lipid peroxidation can also be analyzed as the effect of ROS on polyunsaturated fatty acid oxidation is one of the hallmarks of ferroptosis as well as CHAC1 and PTGS2 genes upregulation which can be validated by qPCR method (Chen et al., 2021).

A pronounced effect of ATO/D-VC can be seen in downregulation of Complex II activity. This leads to subsequent decrease in Complex III and IV enzymatic activity. As electron transport chain is affected it can be tested if ATP production drops as well, and in addition to it the TCA cycle activity may also play part as it supplies ETC with succinate utilized by complex II.

As it was shown, TTFA gives a partial rescue from ATO/D-VC treatment showing that its mechanism of action is highly dependent on complex II activity. To further validate this observation and quantitate it Annexin V/PI staining can be performed in combination with MitoSOX staining which is expected to show the reduction of ROS production under TTFA pretreatment before ATO/D-VC.

In conclusion, the current study indicates that the combination of ATO and D-VC produces high levels of reactive oxygen species, particularly superoxide. This leads to programmed cell death with mitochondrial complex II identified as a key target of the drug combination. However, further research is still needed to reach more comprehensive view on ATO/D-VC mechanism of action.

6 REFERENCES

Begimbetova, D., Burska, A. N., Baltabekova, A., Kussainova, A., Kukanova, A., Fazyl, F., Ibragimova, M., Manekenova, K., Makishev, A., Bersimbaev, R. I., & Sarbassov, D. D. (2024). The Vitamin C Enantiomers Possess a Comparable Potency in the Induction of Oxidative Stress in Cancer Cells but Differ in Their Toxicity. International journal of molecular sciences, 25(5), 2531. https://doi.org/10.3390/ijms25052531

Begimbetova, D., Kukanova, A., Fazyl, F., Manekenova, K., Omarov, T., Burska, A. N., Khamijan, M., Gulyayev, A., Yermekbayeva, B., Makishev, A., Saliev, T., Batyrbekov, K., Aitbayev, C., Spatayev, Z., & Sarbassov, D. (2022). The Oxidative Drug Combination for Suppressing KRAS G12D Inducible Tumour Growth. BioMed research international, 2022, 9426623. https://doi.org/10.1155/2022/9426623

Birch-Machin, M. A., & Turnbull, D. M. (2001). Assaying mitochondrial respiratory complex activity in mitochondria isolated from human cells and tissues. Methods in cell biology, 65, 97–117. https://doi.org/10.1016/s0091-679x(01)65006-4

Bivona, T. G., Quatela, S. E., Bodemann, B. O., Ahearn, I. M., Soskis, M. J., Mor, A., Miura, J., Wiener, H. H., Wright, L., Saba, S. G., Yim, D., Fein, A., Pérez de Castro, I., Li, C., Thompson, C. B., Cox, A. D., & Philips, M. R. (2006). PKC regulates a farnesyl-electrostatic switch on K-Ras that promotes its association with Bcl-XL on mitochondria and induces apoptosis. Molecular cell, 21(4), 481–493. https://doi.org/10.1016/j.molcel.2006.01.012

Burska, A. N., Ilyassova, B., Dildabek, A., Khamijan, M., Begimbetova, D., Molnár, F., & Sarbassov, D. D. (2022). Enhancing an Oxidative "Trojan Horse" Action of Vitamin C with Arsenic Trioxide for Effective Suppression of KRAS-Mutant Cancers: A Promising Path at the Bedside. Cells, 11(21), 3454. https://doi.org/10.3390/cells11213454

Chen, Q., Vazquez, E. J., Moghaddas, S., Hoppel, C. L., & Lesnefsky, E. J. (2003). Production of reactive oxygen species by mitochondria: central role of complex III. The Journal of biological chemistry, 278(38), 36027–36031. https://doi.org/10.1074/jbc.M304854200

Chen, X., Comish, P. B., Tang, D., & Kang, R. (2021). Characteristics and Biomarkers of Ferroptosis. Frontiers in cell and developmental biology, 9, 637162. https://doi.org/10.3389/fcell.2021.637162

Chen, X. Y., Chen, Y., Qu, C. J., Pan, Z. H., Qin, Y., Zhang, X., Liu, W. J., Li, D. F., & Zheng, Q. (2019). Vitamin C induces human melanoma A375 cell apoptosis via Bax- and Bcl-2-mediated mitochondrial pathways. Oncology letters, 18(4), 3880–3886. https://doi.org/10.3892/ol.2019.10686

Chun, S. Y., Johnson, C., Washburn, J. G., Cruz-Correa, M. R., Dang, D. T., & Dang, L. H. (2010). Oncogenic KRAS modulates mitochondrial metabolism in human colon cancer cells by inducing HIF-1α and HIF-2α target genes. Molecular cancer, 9, 293. https://doi.org/10.1186/1476-4598-9-293

Hosseini, M. J., Shaki, F., Ghazi-Khansari, M., & Pourahmad, J. (2013). Toxicity of Arsenic (III) on Isolated Liver Mitochondria: A New Mechanistic Approach. Iranian journal of pharmaceutical research : IJPR, 12(Suppl), 121–138.

Hu, Y., Lu, W., Chen, G., Wang, P., Chen, Z., Zhou, Y., Ogasawara, M., Trachootham, D., Feng, L., Pelicano, H., Chiao, P. J., Keating, M. J., Garcia-Manero, G., & Huang, P. (2012). K-ras(G12V) transformation leads to mitochondrial dysfunction and a metabolic switch from oxidative phosphorylation to glycolysis. Cell research, 22(2), 399–412. https://doi.org/10.1038/cr.2011.145

Kaźmierczak-Barańska, J., Boguszewska, K., Adamus-Grabicka, A., & Karwowski, B. T. (2020). Two Faces of Vitamin C-Antioxidative and Pro-Oxidative Agent. Nutrients, 12(5), 1501. https://doi.org/10.3390/nu12051501

Kim, H. J., Lee, H. N., Jeong, M. S., & Jang, S. B. (2021). Oncogenic KRAS: Signaling and Drug Resistance. Cancers, 13(22), 5599. https://doi.org/10.3390/cancers13225599

Kikuchi, H., Pino, M. S., Zeng, M., Shirasawa, S., & Chung, D. C. (2009). Oncogenic KRAS and BRAF differentially regulate hypoxia-inducible factor-1alpha and -2alpha in colon cancer. Cancer research, 69(21), 8499–8506. https://doi.org/10.1158/0008-5472.CAN-09-2213

Kowaltowski, A. J., de Souza-Pinto, N. C., Castilho, R. F., & Vercesi, A. E. (2009). Mitochondria and reactive oxygen species. Free radical biology & medicine, 47(4), 333–343. https://doi.org/10.1016/j.freeradbiomed.2009.05.004

Liberti, M. V., & Locasale, J. W. (2016). The Warburg Effect: How Does it Benefit Cancer Cells?. Trends in biochemical sciences, 41(3), 211–218. https://doi.org/10.1016/j.tibs.2015.12.001

Luo J. (2021). KRAS mutation in pancreatic cancer. Seminars in oncology, 48(1), 10–18. https://doi.org/10.1053/j.seminoncol.2021.02.003

Mo, S. P., Coulson, J. M., & Prior, I. A. (2018). RAS variant signalling. Biochemical Society transactions, 46(5), 1325–1332. https://doi.org/10.1042/BST20180173

Moindjie, H., Rodrigues-Ferreira, S., & Nahmias, C. (2021). Mitochondrial Metabolism in Carcinogenesis and Cancer Therapy. Cancers, 13(13), 3311. https://doi.org/10.3390/cancers13133311

Molina, J. R., & Adjei, A. A. (2006). The Ras/Raf/MAPK pathway. Journal of thoracic oncology : official publication of the International Association for the Study of Lung Cancer, 1(1), 7–9.

Neuzil, J., Rohlena, J., & Dong, L. F. (2012). K-Ras and mitochondria: dangerous liaisons. Cell research, 22(2), 285–287. https://doi.org/10.1038/cr.2011.160

Ngo, B., Van Riper, J. M., Cantley, L. C., & Yun, J. (2019). Targeting cancer vulnerabilities with high-dose vitamin C. Nature reviews. Cancer, 19(5), 271–282. https://doi.org/10.1038/s41568-019-0135-7

Read, A. D., Bentley, R. E., Archer, S. L., & Dunham-Snary, K. J. (2021). Mitochondrial iron-sulfur clusters: Structure, function, and an emerging role in vascular biology. Redox biology, 47, 102164. https://doi.org/10.1016/j.redox.2021.102164

Ros, J., Vaghi, C., Baraibar, I., Saoudi González, N., Rodríguez-Castells, M., García, A., Alcaraz, A., Salva, F., Tabernero, J., & Elez, E. (2024). Targeting KRAS G12C Mutation in Colorectal Cancer, A Review: New Arrows in the Quiver. International journal of molecular sciences, 25(6), 3304. https://doi.org/10.3390/ijms25063304

Salscheider, S. L., Gerlich, S., Cabrera-Orefice, A., Peker, E., Rothemann, R. A., Murschall, L. M., Finger, Y., Szczepanowska, K., Ahmadi, Z. A., Guerrero-Castillo, S., Erdogan, A., Becker, M., Ali, M., Habich, M., Petrungaro, C., Burdina, N., Schwarz, G., Klußmann, M., Neundorf, I., Stroud, D. A., … Riemer, J. (2022). AIFM1 is a component of the

mitochondrial disulfide relay that drives complex I assembly through efficient import of NDUFS5. The EMBO journal, 41(17), e110784. https://doi.org/10.15252/embj.2022110784

Schieber, M., & Chandel, N. S. (2014). ROS function in redox signaling and oxidative stress. Current biology : CB, 24(10), R453–R462. https://doi.org/10.1016/j.cub.2014.03.034

Spinazzi, M., Casarin, A., Pertegato, V., Salviati, L., & Angelini, C. (2012). Assessment of mitochondrial respiratory chain enzymatic activities on tissues and cultured cells. Nature protocols, 7(6), 1235–1246. https://doi.org/10.1038/nprot.2012.058

Vafa, O., Wade, M., Kern, S., Beeche, M., Pandita, T. K., Hampton, G.M., & Wahl, G. M. (2002). c-Myc can induce DNA damage, increase reactive oxygen species, and mitigate p53 function: a mechanism for oncogene-induced genetic instability. Molecular cell, 9(5), 1031–1044. https://doi.org/10.1016/s1097-2765(02)00520-8

Wang, Y., Kaiser, C. E., Frett, B., & Li, H. Y. (2013). Targeting mutant KRAS for anticancer therapeutics: a review of novel small molecule modulators. Journal of medicinal chemistry, 56(13), 5219–5230. https://doi.org/10.1021/jm3017706

Warburg, O. (1925). The Metabolism of Carcinoma Cells. The Journal of Cancer Research, 9(1), 148–163. https://doi.org/10.1158/jcr.1925.148

Warburg, O. (1956). On the Origin of Cancer Cells. Science, 123(3191), 309-314. https://doi.org/10.1126/science.123.3191.309

Wu, X., Park, M., Sarbassova, D. A., Ying, H., Lee, M. G., Bhattacharya, R., Ellis, L., Peterson, C. B., Hung, M. C., Lin, H. K., Bersimbaev, R. I., Song, M. S., & Sarbassov, D. D. (2020). A chirality-dependent action of vitamin C in suppressing Kirsten rat sarcoma mutant tumor growth by the oxidative combination: Rationale for cancer therapeutics. International journal of cancer, 146(10), 2822–2828. https://doi.org/10.1002/ijc.32658

Yu, C., Min, S., Lv, F., Ren, L., Yang, Y., & Chen, L. (2023). Vitamin C inhibits the growth of colorectal cancer cell HCT116 and reverses the glucose-induced oncogenic effect by downregulating the Warburg effect. Medical oncology (Northwood, London, England), 40(10), 297. https://doi.org/10.1007/s12032-023-02155-x

Zhao, R. Z., Jiang, S., Zhang, L., & Yu, Z. B. (2019). Mitochondrial electron transport chain, ROS generation and uncoupling (Review). International journal of molecular medicine, 44(1), 3–15. https://doi.org/10.3892/ijmm.2019.4188

Zheng, H., Xu, Y., Liehn, E. A., & Rusu, M. (2024). Vitamin C as Scavenger of Reactive Oxygen Species during Healing after Myocardial Infarction. International journal of molecular sciences, 25(6), 3114. https://doi.org/10.3390/ijms25063114

7 APPENDICES

Supplementary table 1. Annexin V/PI staining in AK192 cell line in control (GM) and under ATO/D-VC treatment (mean value from three independent experiments each in triplicate).

	A-/PI-	A+/PI-	A+/PI+	A-/PI+
GM (24H)	86.28%	3.14%	10.23%	0.35%
ATO/D-VC (24H)	61.3%	5.02%	32.74%	0.94%
GM (48H)	62.45%	5.81%	30.9%	0.84%
ATO/D-VC (48H)	11.52%	2.86%	81.01%	4.61%

Supplementary table 2. Annexin V/PI staining in HCT116 cell line in control (GM) and under ATO/D-VC treatment (mean value from three independent experiments each in triplicate).

	A-/PI-	A+/PI-	A+/PI+	A-/PI+
GM (24H)	89.277%	3.67%	6.427%	0.61%
ATO/D-VC (24H)	83.062%	4.952%	10.988%	1.002%
GM (48H)	88.09%	5.487%	6.277%	0.143%
ATO/D-VC (48H)	26.483%	6.245%	66.568%	0.708%

Supplementary table 3. Percentage of MitoSOX positive cells in AK192 and HCT116 cell lines in control (GM) and under ATO/D-VC treatment (mean value from three independent experiments each in triplicate).

	GM (24H)	ATO/D-VC (24H)	GM (48H)	ATO/D-VC (48H)
AK192	7.09%	54.88%	11.34%	76.89%
HCT116	2.84%	7.49%	3.85%	49.23%

Supplementary table 4. Electron transport chain activity in nmon/min/mg in AK192 cell line at 24 hours post treatment (mean value from three independent experiments each in triplicate).

Complex I		**Complex II**		**Complex III**		**Complex IV**	
GM	ATO/D-VC	GM	ATO/D-VC	GM	ATO/D-VC	GM	ATO/D-VC
527.33	235.9	141.76	52.88	413.38	197.38	702.70	688.23
332.26	269.71	112.7	43.48	415.70	195.47	675.47	693.6
189.71	464.33	127.94	51.83	359.33	187.55	634.42	686.75
		106.64	49.74	203.61	92.65	767.24	736.59
		110.65	42.63	195.05	122.25	776.27	787.29
		145.99	63.21	158.18	124.72	738.55	702.85
		132.25	66.59	427.37	86.10	867.25	776.34
		137.78	65.01	352.19	82.12	862.67	622.39
			64.26		74.15	874.39	604.32
							563.22
							611.94

Supplementary table 5. Electron transport chain activity in nmon/min/mg in HCT116 cell line at 48 hours post-treatment (mean value from three independent experiments each in triplicate).

Complex I		**Complex II**		**Complex III**		**Complex IV**	
GM	ATO/D-VC	GM	ATO/D-VC	GM	ATO/D-VC	GM	ATO/D-VC
499.02	541.93	68.35	41.46	308.17	239.73	500.18	451.65
456.22	598.25	65.97	47.4	278.37	242.7	506.13	441.54
491.71	385.73	58.75	41.61	263.61	206.49	463.96	451.47
	320.91	68.63	54.81	251.36	273.28	516.76	395.29
		75.67	54.58	243.24	255.76	550.73	443.02
		73.52	55.64	199.17	247.82	562.2	494.14
			62.87	189.73	224.64	554.19	486.89
			56.64			578.94	547.97
			53.45			478.9	387.53
						481.06	339.7
						461.47	363.98